SWIN
BUR
NE

SWINBURNE UNIVERSITY
OF TECHNOLOGY

Core radius evolution of star clusters

M. I. Wilkinson[1], J. R. Hurley[2], A. D. Mackey[1], G. Gilmore[1], C. A. Tout[1]

[1] *Institute of Astronomy, Madingley Rd, Cambridge CB3 0HA*
[2] *Department of Astrophysics,American Museum of Natural History,Central Park West at 79th Street, New York, NY 10024, USA*

arXiv:astro-ph/0304522v1 29 Apr 2003

ABSTRACT

We use N-body simulations of star clusters to investigate the possible dynamical origins of the observed spread in core radius among intermediate-age and old star clusters in the Large Magellanic Cloud (LMC). Two effects are considered, a time-varying external tidal field and variations in primordial hard binary fraction. Simulations of clusters orbiting a point-mass galaxy show similar core radius evolution for clusters on both circular and elliptical orbits and we therefore conclude that the tidal field of the LMC has not yet significantly influenced the evolution of the intermediate-age clusters. The presence of large numbers of hard primordial binaries in a cluster leads to core radius expansion; however, the magnitude of the effect is insufficient to explain the observations. Further, the range of binary fractions required to produce significant core radius growth is inconsistent with the observational evidence that all the LMC clusters have similar stellar luminosity functions.

Key words: galaxies: Magellanic Clouds, star clusters - globular clusters: general

1 INTRODUCTION

Star clusters are vital laboratories for testing theories of stellar dynamics and stellar evolution (e.g. Meylan & Heggie 1997). The globular clusters orbiting the Milky Way constitute a sample of about 150 evolved stellar systems with ages $\gtrsim 10^{10}$ years. These provide useful constraints on the long term evolution of clusters but information about the paths which led to these end states can only be inferred via comparisons with the end points of numerical cluster simulations. In contrast, the system of rich star clusters in the Large Magellanic Cloud (LMC) includes clusters of comparable mass to Galactic globular clusters but which span the entire age range from less than 5×10^6 years (e.g. R 136) to about 10^{10} years (e.g. NGC 2019). This allows us to observe massive star clusters at various epochs in their evolution and makes it possible to identify evolutionary trends, under the assumption that the external processes affecting cluster evolution have not changed significantly over the lifetime of the LMC. With this aim in mind, HST project GO7307 (e.g. Beaulieu et al. 1999) obtained deep images of four pairs of LMC clusters. Within each selected pair the clusters are approximately coeval, have similar masses and metallicities and lie at comparable radii from the LMC centre but differ significantly in other properties such as core radius. The pairs range in age from about 10^7 years up to 10^{10} years. The youngest clusters (NGC 1805 and NGC 1818) are old enough to have expelled all their residual gas and so are pure N-body systems.

Fig. 1 shows a plot of the observed core radii of star clusters in the LMC as a function of their ages, with the clusters in the GO7307 HST sample identified by name. There is a clear trend that the spread in core radius is an increasing function of cluster age. This trend was first identified by Elson et al. (1989) from ground-based images and was recently confirmed by Mackey & Gilmore (2003) using HST archive data. Mackey & Gilmore (2003) calculated core radii for 53 LMC clusters in a uniform manner with the aim of obtaining an unbiased data set. They discuss in some detail the uncertainties in the data and conclude that selection effects are not responsible for the observed trend. They suggest, as Elson et al. (1989) had earlier argued, that the increased spread in core radius is an evolutionary phenomenon: all clusters formed with relatively small core radii ($\sim 2 - 3$ pc) and subsequently some clusters experienced core expansion while others did not.

Elson et al. (1989) discuss the possibility that intercluster variations in the slope of the initial mass function (IMF) could have produced the observed spread in core radius. They point out that mass loss from the increased numbers of massive stars found in clusters with IMFs flatter than the standard Salpeter IMF could lead to core expansion of the observed magnitude on a timescale of about $10^{8.5}$ years. As Elson (1991) notes, however, the IMF slope required to explain the largest core radii would lead to disruption of the clusters on a timescale of a few $\times 10^7$ years. More directly, based on a detailed observational analysis of the clusters in the GO7307 HST sample, de Grijs et al. (2002b) have shown that the slopes of their luminosity functions are similar to each other within the observational uncertainties, strongly

suggesting that their IMFs were very similar down to stellar masses of about $0.8 - 1.0 M_\odot$. The absence of inter-cluster population variations implies that stellar evolutionary mass loss cannot be invoked to explain the observations.

As a star cluster evolves, encounters lead to a redistribution of energy among the stars. Heavier stars and binaries acquire lower velocities, on average, and sink towards the cluster core. This process of mass segregation could enhance the heating effect of a population of primordial binaries because the binaries would tend to fall to the centre where encounters occur more frequently. Observations of young clusters (e.g. Hillenbrand 1997) and numerical simulations of star formation (e.g. Bonnell et al. 2001) show that so-called primordial mass segregation can also result from the cluster formation process. de Grijs et al. (2002b) have shown that there is strong evidence for mass segregation in all the young and intermediate-age clusters in the GO7307 sample. Further, the amount of mass segregation appears to be similar in all clusters and cannot therefore account for differences in the cluster core radii.

The aim of this paper is to investigate, by means of N-body simulations, whether dynamical processes could give rise to the observed core radius–age relation. In this context, the pair of clusters NGC 1868 and NGC 1831 are of particular interest. These clusters have very similar ages and metallicities and their masses differ by at most a factor of two (see Table 1 of de Grijs et al. 2002b). However, as Fig. 1 shows, the core radius of NGC 1831 is almost three times larger than that of NGC 1868. Given that the cluster ages are only around 500 Myr any process which has affected the core radii must be capable of producing significant evolution even on this relatively short time scale. In this paper, we consider the dynamical effects of (1) variations in the external tidal field experienced by the clusters and (2) differences in the initial numbers of dynamically active binary stars in the clusters. Given that the crossing times at the half-mass radii of these clusters are about 10^7 yrs and the times to orbit the LMC are about the same order of magnitude, it is reasonable to suppose that either of these processes could have begun to produce observable effects on cluster structure on the relevant time scale.

During the past decade, numerical simulations of star clusters have become increasingly realistic owing to dramatic increases in computational speeds and significant improvements in programming algorithms (e.g. Aarseth 1999). The N-body code used in this paper incorporates the stellar evolution models of Hurley et al. (2000, 2002). This makes it possible to analyse the output from the simulations in an identical manner to that used for observational data, thus allowing meaningful confrontation of models with observations. This is particularly important when discussing cluster properties such as core radius because the relation between the theoretical and observational definitions of this quantity depend on the conversion between the mass function and luminosity function of the cluster stars. For a real cluster this conversion is non-trivial because it depends on, among other quantities, the cluster metallicity and is further complicated by the possible presence of mass segregation (see e.g. de Grijs et al. 2002a). In this paper, all comparisons between models and observations are made in terms of directly observable properties.

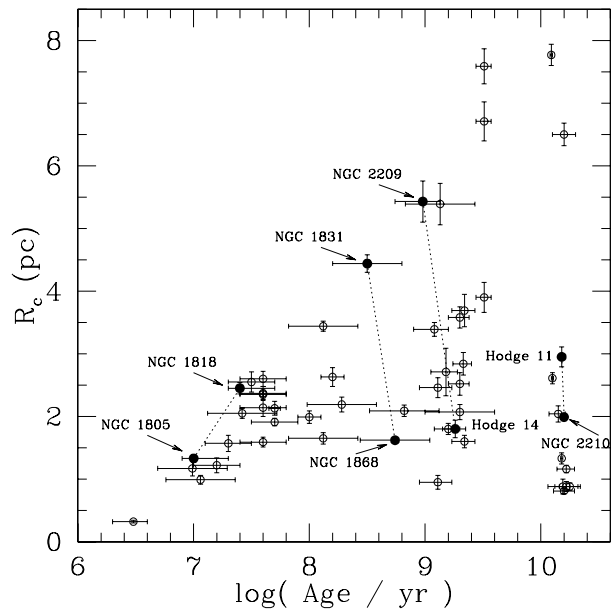In the interests of clarity, we include here a note on the

Figure 1. Observed core radii R_c of LMC star clusters as a function of age. The clusters in the GO7307 HST sample are identified by name, and matched pairs are joined by dotted lines. (Following Fig. 1 of de Grijs et al. (2002b), data taken from Mackey & Gilmore (2003)).

definition of the core radius. As Casertano & Hut (1985) discuss, theoreticians, numerical simulators and observers assign different meanings to the term "core radius", reflecting the quantity of greatest relevance to their purpose. In theoretical work, the core radius r_c refers to the natural length scale of the system under study, for example the scale radius of the widely used King (1966) profile. The operational definition of the core radius commonly used in discussions of N-body simulations is that of the density radius r_d. This is the density-weighted average of the distance of each star from the density centre (Aarseth 2001), where the local density at each star is estimated from the mass within a sphere containing the star's six nearest neighbours and the density centre is defined as the density-weighted mean position of the stars. Observationally, since the available information is either in the form of cluster surface brightness profiles or luminosities of individual stars instead of mass densities and stellar masses, the core radius R_c corresponds to the radius at which the projected surface brightness falls to half its central value. In the case of a cluster of equal-mass stars in equilibrium, there is generally a well-defined relation between r_c and R_c. For example, for a Plummer (1911) model it is straightforward to show that $R_c = 0.6435 r_c$. It is important to note, however, that during the evolution of the cluster this relation is not static and that there is no general relation between r_d and either r_c or R_c. In this paper, we use the term "core radius" exclusively to refer to the observational quantity R_c. In Section 3.4 we will compare the evolution of r_d and R_c, in order to emphasize the care which must be taken in comparing observations with simulations.

In Section 2 we describe briefly the N-body code used in the simulations, as well as the pipeline used to calculate observational properties of the simulated clusters. Section 3

Table 1. Summary of N-body runs performed. N_0, M_0 and $f_{b,0}$ are the initial number of stars, total stellar mass and primordial fraction of hard binaries, respectively. The clusters were all simulated in the tidal field of a point mass representing the LMC, and each simulation ran until time T_{max}.

Name	N_0	M_0 (M$_\odot$)	$f_{b,0}$	Orbit	T_{max}
Circ	5000	2390	0	Circular	1.0 Gyr
Ecc	5000	2410	0	Elliptical	1.0 Gyr
Binary	4500	2310	0.5	Circular	1.7 Gyr
Binary2	4500	2390	0.25	Circular	1.6 Gyr
Binary3	4500	2180	0.1	Circular	1.0 Gyr
BinaryEcc	4500	2340	0.5	Elliptical	1.6 Gyr

considers the effects of time variation of an external tidal field on the evolution of the cluster core radius while Section 4.1 deals with clusters moving in a steady tidal field but with different initial binary fractions. In Section 4.2 we investigate the combined effect of both mechanisms by studying binary-rich clusters in a time-varying tidal field and the results of these simulations are discussed in the context of the LMC clusters in Section 4.3. Finally in Section 5 we summarise our conclusions.

2 N-BODY SIMULATIONS

N-body simulations are a very valuable tool in the study of star clusters because they allow many different processes to be studied with a minimum of simplifying assumptions. The simulations discussed below were performed using the NBODY4 code (e.g. Aarseth 1999) running on the HARP-3 and GRAPE-6 special purpose computers (Makino et al. 1997) at the Institute of Astronomy, Cambridge and on a GRAPE-6 board at the American Museum of Natural History. The NBODY4 code uses the 4th order Hermite integration scheme to follow the orbits of the cluster stars and utilises state-of-the-art regularisation schemes (Mikkola & Aarseth 1993, 1998) for the accurate and efficient treatment of the internal motion of binary and higher-order subsystems. It also incorporates a full set of stellar evolution models, in the form of parameterized functions, which are used to follow the evolution of single stars and binaries (Hurley et al. 2001). Of particular importance to the present study is the treatment of mass loss. Any gas which is lost from an evolving star and is not accreted on to a binary companion is assumed to leave the cluster instantaneously, thereby reducing the depth of the cluster potential well. A realistic treatment of mass loss is therefore essential to allow the study of the evolution of such cluster properties as the core radius.

Within the N-body code the equations of motion are integrated in scaled units such that $G = 1$ and the total mass and virial radius of the cluster are also set to unity (Heggie & Mathieu 1986). For a star cluster in virial equilibrium the initial energy in these units is $-1/4$ and the crossing time is $2\sqrt{2}$. Given the total mass of the cluster in solar masses and an appropriately chosen length scale (which determines the conversion from N-body length units to physical units) it is straightforward to obtain the conver-

sion factors for time and velocity from N-body units to Myr and km s^{-1}, respectively.

In order to facilitate direct comparison of the results of our simulations with the observed data, we determine the core radius for each model cluster using the same processing pipeline as that used by Mackey & Gilmore (2003). In summary, the stellar data from the model clusters (in the form of position and luminosity information for each member star) are binned radially to obtain a projected surface brightness profile. The three-parameter model (Elson et al. 1987)

$$\mu(r) = \mu_0 \left(1 + \frac{r^2}{a^2}\right)^{-\frac{\gamma}{2}} \tag{1}$$

is then fitted to the cluster profile. Here, μ_0 is the central surface brightness, γ determines the fall-off of the surface brightness profile at large radii and R_c is related to the length scale a via $R_c = a(2^{2/\gamma} - 1)^{1/2}$. Full details of the fitting procedure used and discussion of the associated uncertainties are presented in Mackey & Gilmore (2003). In order to reduce the numerical noise due to the small number of stars in our simulated clusters we observe each cluster along three perpendicular lines of sight and obtain the median core radius from these three estimates. This helps to reduce the impact of individual bright stars which might otherwise skew the core radius estimation. Further, each N-body run is performed four times using different random realisations of the initial cluster model and the results are averaged in order to ensure the robustness of any observed trends.

Initially, all the model clusters are generated according to a Plummer (1911) density law

$$\rho(r) = \frac{\rho_0 r_P^5}{(r_P^2 + r^2)^{5/2}}, \tag{2}$$

following the prescription of Aarseth et al. (1974). Here r_P is the Plummer length scale and ρ_0 is the central mass density. Observations of the young clusters in the LMC show that they do not appear to be tidally limited (Mackey & Gilmore 2003). In this case, the Plummer profile is a reasonable model to use for the initial density profile given that the fall-off in its outer regions lies between that of a tidally truncated King model and the observed profiles of the young LMC clusters.

The initial distribution of stellar masses is drawn from the IMF of Kroupa et al. (1993) which is a three-part power law fit to stellar data in the solar neighbourhood. We take the lower and upper mass limits to be 0.1M$_\odot$ and 50M$_\odot$, respectively. We assume solar metallicity for the stars in our clusters. This is an appropriate choice for the younger clusters – for example, Johnson et al. (2001) have shown that NGC 1805 and NGC 1818, whose ages are about 10 and 25 Myr respectively, are well matched by isochrones of approximately solar metallicity. Since the pairs of clusters in the GO7307 HST sample were chosen to have similar metallicity, we know a priori that the observed range of cluster core radii cannot be due to metallicity variations. We have therefore chosen to perform all our simulations at solar metallicity, and postpone discussion of the effects of metallicity variations on star cluster evolution to future work.

Table 1 summarises the simulations which we have performed. The clusters in these runs initially contain 4500 or 5000 stars and have a mean mass of about 2300 M$_\odot$. Clearly,

the LMC clusters are more massive and contain greater numbers of stars than our model clusters and therefore direct comparison of the results of our simulations with the observed data must be approached with caution. However, the effects of increasing N in our simulations can be estimated by considering the various time scales in the problems we study. Detailed discussion of these scaling issues is presented in Sections 3.4 and 4.3 where we argue that none of our conclusions is strongly dependent on the small size of our simulated clusters.

3   TIME-VARYING TIDAL FIELDS

3.1   Model Initialisation

We first consider the effects of the external tidal field of the LMC on the evolution of the cluster core radii. Theoretical arguments and numerical simulations strongly suggest that tides have played a significant role in the evolution of star clusters and cluster systems in galaxies such as the Milky Way (e.g. Gnedin & Ostriker 1997; Vesperini & Heggie 1997; Vesperini 1998; Baumgardt 1998; Fall & Zhang 2001) . In addition, observations of tidal tails around at least twenty Milky Way globular clusters (e.g. Leon et al. 2000; Odenkirchen et al. 2001) provide compelling evidence of the ongoing disruption of star clusters by the Milky Way. The gravitational field of the LMC (mass $\approx$ $10^{10} M_\odot$) is much weaker than that of a galaxy like the Milky Way (mass $\approx$ $10^{12} M_\odot$). However, as Mackey & Gilmore (2003) show (their Fig. 15), there is a deficit of low-mass clusters older than 10^{10} years. If we assume that the cluster population originally contained a spectrum of cluster masses similar to that of the present-day young clusters, their absence at late times strongly suggests that tides have been at work on the cluster system in exactly the manner expected from the models of Gnedin & Ostriker (1997). Given that the GO7307 HST sample of 8 clusters was selected on the basis that they lie at similar distances from the LMC centre but display a wide range of core radii, the steady tidal field experienced by a cluster on a roughly circular orbit cannot be the origin of the observed trends. Further, given the intrinsic weakness of the LMC field at a radius of 4 kpc, where our clusters lie, one might not expect the tidal field to play a significant role in cluster evolution. We therefore consider clusters on non-circular orbits. Such clusters experience tidal shocks during their orbits and we investigate whether these impart sufficient energy to the cluster to produce differences in the evolution of R_c. Elson (2000) discusses the possible role of disk shocking in the internal evolution of the intermediate-age LMC clusters, but questions whether any of the clusters is on an appropriate disk-crossing orbit for this to be an important effect. In this section we consider instead the tidal shocking produced by a point mass galaxy.

In order to investigate the role of the LMC tidal field in the evolution of its cluster system, it is necessary to incorporate an appropriate external gravitational field into the simulations. We model the LMC potential as that of a point mass of $9 \times 10^9 M_\odot$. This is a rather drastic oversimplification of the actual situation. We note, however, that this model exaggerates the effect of the tidal field, as any extended distribution of mass will have a more slowly varying gravitational potential. Further, in the radius range $2 - 8$ kpc, in

which our model clusters orbit, the gradient of the potential is within a factor of two of that of the detailed LMC mass model of van der Marel et al. (2002). Thus our simulations constitute a plausible upper limit to the possible effects of tides.

In the N-body simulations, the equations of motion are integrated in an accelerating but non-rotating reference frame centred on the centre of mass of the cluster and whose axes are aligned with fixed spatial directions. This choice of frame simplifies the equations of motion for a cluster on a non-circular orbit despite having less symmetry than the more usual rotating frame used for steady tidal fields whose axes always point towards the attracting centre (Heggie 2001). Implementation of the time varying tidal field requires some care because mass loss from evolving stars or the escape of stars from the cluster causes the centre of mass to acquire a non-zero velocity relative to the frame of integration. It is therefore necessary to re-centre the frame of reference to coincide with the rest frame of the centre of mass following each such event. All internal and external forces must then be reinitialized to ensure consistency with the re-centred frame during subsequent integrations.

We have performed simulations for clusters on elliptical orbits with perigalactic radii $R_p \approx 2$ kpc and apogalactic radii $R_a \approx 8$ kpc, probing the region in which most of our sample clusters lie but largely avoiding the complications of the inner regions of the LMC which may contain a stellar bar (e.g. Zhao & Evans 2000). We also modelled clusters on circular orbits at a radius of 6 kpc which corresponds to the time-averaged radius of the elliptical orbits. This allows us to isolate the effect of the time variation of the tidal field because both sets of clusters experience the same mean tidal field.

We calculate the initial perigalactic tidal radius $r_{t,p}$ in the approximation that the cluster is on a circular orbit at a radius R_p. In this case, $r_{t,p}$ is determined from the cluster mass M, the mass of the point mass galaxy M_G and R_p via (e.g. King 1962)

$$r_{t,p} = R_p \left(\frac{M}{3GM_G} \right)^{1/3}. \tag{3}$$

The apocentric tidal radius $r_{t,a}$ is determined in a similar way from R_a. The unit of length, which determines the conversion between N-body length units and physical units, is then chosen such that the limiting radius of all clusters is initially equal to $r_{t,p}$. However, at the start of the simulations the clusters are placed at the apocentre of their orbits about the LMC which means that they do not fill their tidal radii. If, instead, the clusters initially extended to $r_{t,a}$ and were not truncated at $r_{t,p}$ then the removal of stars outside $r_{t,p}$ during the first few perigalactic passages could mask any heating effects at radii interior to $r_{t,p}$ due to the time variation of the tidal field. In contrast to a King model, the Plummer density law (2) formally extends to infinity and so the outer radius of a cluster is not well-defined. The length unit we use yields a pericentric tidal radius close to the (random) position of the outermost star in our initial clusters. The internal stellar velocities are scaled to ensure virial equilibrium at the start of the simulation.

The tidal radius of a cluster on an elliptical orbit does not have a unique value. It varies continuously both as the cluster moves along its orbit and when the cluster loses mass

through stellar evolution or the escape of member stars. However, for clusters whose internal relaxation times are longer than their orbital periods, tidal stripping tends to truncate the star cluster at $r_{t,p}$ (Oh & Lin 1992). These two time scales are of similar magnitude for our simulated clusters so we expect two-body relaxation processes to lead to some expansion of the cluster beyond $r_{t,p}$. We take account of this by defining escaping stars to be those stars outside twice the apogalactic tidal radius $r_{t,a}$. Stars whose orbits carry them outside this radius are generally lost to the cluster (e.g. Heggie 2001). Stars are thus free to populate the region between $r_{t,p}$ and $2r_{t,a}$.

The choice of length unit determines the physical density of the cluster and hence the physical rate at which two-body relaxation processes affect the evolution of the cluster. Our aim is to investigate the influence of a time-varying external tidal field so it is important to ensure that all internal evolutionary processes proceed in an identical manner for each of our simulated clusters. We therefore use the same length unit for the clusters on circular orbits as we chose for those on elliptical orbits. This means that the clusters on circular orbits also do not initially fill their tidal radii and so necessarily allows expansion of these clusters. However, since the circular orbits are placed at the time-averaged radius of the elliptical orbits this expansion should on average be the same for both sets of clusters. Any differences in the rates of expansion are due to the time variation in the tidal field.

The effect of steady tidal fields on star cluster evolution has been the subject of papers by a number of authors (e.g. Giersz & Heggie 1997; Aarseth & Heggie 1998; Baumgardt 2001; Portegies Zwart et al. 2002). However, until recently the problem of clusters moving in time-varying tidal fields had received relatively little attention from N-body simulations. Baumgardt (1998) uses the results of some simulations of single-mass star clusters orbiting a point mass to determine the appropriate choice of escape radius for simulations of mass loss. More recently, Baumgardt & Makino (2003) presented an extensive survey of the dynamical evolution of star clusters in external tidal fields. Our investigation is complementary to theirs because we are looking at the evolution of the observable global structure of the cluster while Baumgardt & Makino (2003) focus their attention mostly on the evolution of the stellar mass function within the cluster. The results of all our simulations are presented in terms of quantities which can be compared directly with those calculated from the observed data, thereby enabling us to discuss how different dynamical processes impact on observations.

We follow the evolution of the clusters for about $5\,t_{rh}$ (where t_{rh} is the half-mass relaxation time) This corresponds to $T_{max} \approx 1\,\mathrm{Gyr}$ in most cases. By this time, the clusters on elliptical orbits have lost more than 50 per cent of their stars making estimates of properties such as the core radius increasingly noisy. At regular intervals during the evolution, the data from the clusters are recorded and all relevant properties of the clusters are calculated.

3.2 Results

The solid curve in Fig. 2 presents the evolution of the core radius for clusters on circular orbits about the LMC at a
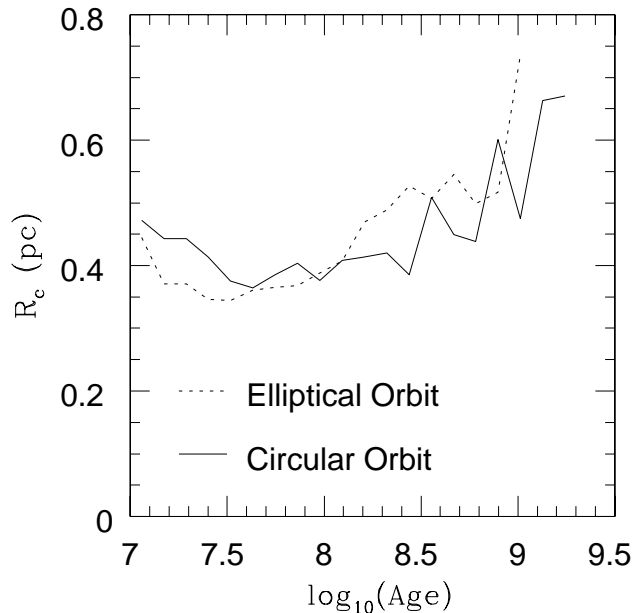

Figure 2. Core radius evolution for N-body simulations of clusters on orbits about a point mass representing the LMC. See text for discussion.

distance of about $6\,\mathrm{kpc}$ from the centre. The broken curve shows the evolution of R_c for clusters on elliptical orbits with the same time-averaged galactocentric radius. It is apparent from this figure that the core radius evolution in both cases is indistinguishable, especially in view of the noise associated with the output of small-N simulations. During the first 10^8 yrs, the core radius is seen to decrease slightly from its initial value. This is because the calculation of R_c is dominated by the light of the most massive stars which rapidly become more centrally concentrated due to the effects of mass segregation. As Fig. 3 shows, after $10.5\,\mathrm{Myr}$ the half-mass radius of the more massive stars is already 30 per cent smaller than that of the less massive stars.

After its initial contraction phase, the core radius begins to increase. This occurs because the clusters do not fill the tidal radius corresponding to their galactocentric positions at the start of the simulations. A combination of mass loss from the rapid evolution of massive stars and two-body relaxation can therefore drive the overall expansion of the cluster seen in Fig. 3. The top panel of Fig. 4 shows that the cluster's half-mass radius r_h is increasing with time (see fourth panel of Fig. 5 for long-term r_h behaviour). During this period its r_d (not shown) is roughly constant at about $0.3\,\mathrm{pc}$.

The expansion of r_h is driven by a combination of two processes which are illustrated in the lower panels of Fig. 4. The middle panel shows the evolution of the virial ratio Q. Initially the cluster is in equilibrium with $Q = 0.5$. After about $10\,\mathrm{Myr}$, the cluster is temporarily displaced from equilibrium ($Q > 0.5$) by mass loss from the most massive stars. This is accompanied by the increase in the half-mass radius of the cluster shown in the top panel of Fig. 4. It is interesting to note that the R_c of the cluster does not change as a result of this mass loss. Stellar evolution cannot account for the sustained expansion of the cluster, however. The cluster loses about 5 per cent of its mass as a result of the above
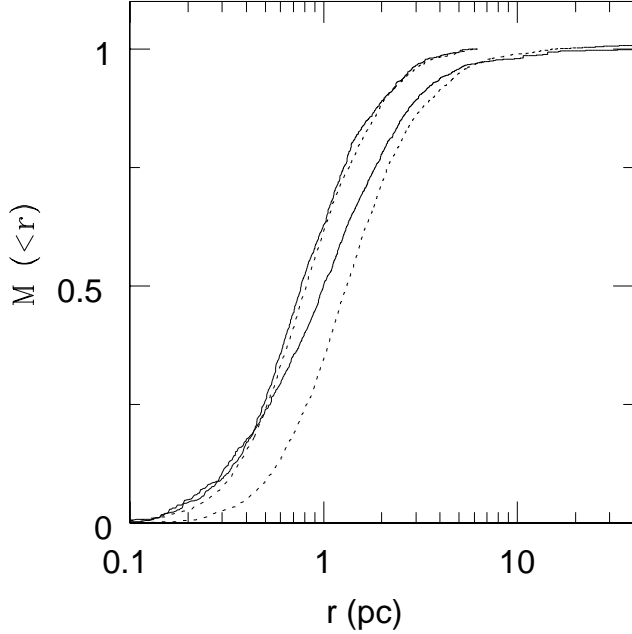
Figure 3. Cumulative mass profiles for stars above (solid curves) and below (broken curves) the median stellar mass for a simulated cluster containing only single stars and on a circular orbit about the LMC. Profiles at two different times are shown: $T = 0$ (upper curves) and $T = 10.5\,\mathrm{Myr}$ (lower curves). There is clear evidence for mass segregation developing in the cluster.

mass loss events. Using the virial theorem it is straightforward to show that the gravitational radius R' of a stellar system with initial radius R and mass M which loses an amount of mass m is given by (Hills 1980)

$$R' = \frac{1}{2}\left(\frac{M-m}{\frac{1}{2}M-m}\right)R. \qquad (4)$$

A 5 per cent mass loss should lead to an increase of less than 10 per cent in the size of the cluster which is insufficient to account for the cluster expansion seen in Figs. 2 and 3.

The bottom panel of Fig. 4 shows the evolution of the velocity anisotropy parameter $\beta = 1 - \langle v_t^2 \rangle / 2 \langle v_r^2 \rangle$ (Binney & Tremaine 1987) inside the 10 per cent Lagrangian radius of the cluster (the radius containing 10 per cent of the total mass of the cluster) and in the outer parts (between the 80 per cent and 90 per cent Lagrangian radii). Initially, the velocity distribution throughout the cluster is isotropic ($\beta = 0$). While the central parts of the cluster retain this isotropy, in the outer parts the distribution becomes increasingly radially anisotropic ($\beta > 0$). This indicates that the continued growth of r_h is being fueled by encounters in the inner parts of the cluster which produce a population of stars on extended radial orbits. The velocity distribution in the outer parts of isolated clusters simulated by Baumgardt et al. (2002) exhibited similar behaviour during post core-collapse evolution; those authors similarly concluded that the growth of the outer Lagrangian radii at late times was due to two-body processes in the inner regions.

Given the similarity between the core radius evolution of clusters on circular and elliptical orbits, we now proceed to investigate the extent to which the clusters on elliptical
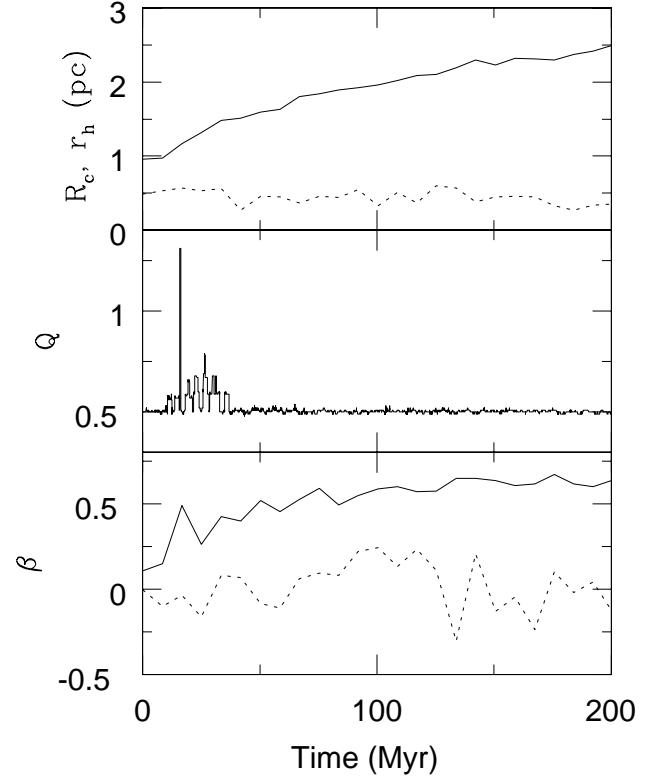

Figure 4. Early evolution of the velocity structure of a cluster on a circular orbit. Top: evolution of the half-mass radius r_h (solid curve) and core radius R_c (broken curve); Middle: plot of the virial ratio Q (whose equilibrium value is 0.5); Bottom: velocity anisotropy parameter β of stars within the inner 10 per cent Lagrangian radius (broken curve) and between the 80 per cent and 90 per cent radii (solid curve). See text for discussion.

orbits have been affected by the variation in the tidal field. Fig. 5 presents the evolution of certain key internal properties of two typical clusters, one on a circular orbit and one on an elliptical orbit. The top panel shows the galactocentric radius R_g along the elliptical orbit to emphasize the clear correlation between perigalactic passages and changes in the internal properties of the cluster on the elliptical orbit. The second panel shows that, as expected, during a perigalactic passage the rms velocity v_rms of the stars in the cluster increases sharply. This velocity kick ejects the most energetic stars from the cluster. As a result of this mass loss, v_rms settles to a value slightly below that of the cluster on the circular orbit once it returns to virial equilibrium.

The third and fourth panels of Fig. 5 show how t_rh and r_h evolve during the cluster orbit. The most noticeable effect is that the relaxation time for the cluster on the elliptical orbit is significantly reduced after the second perigalactic passage, so that the cluster evolves more rapidly following this encounter. This is due both to the decrease in the total number of stars in the cluster and to the increase in the mean stellar mass $\overline{m}$ (shown in the bottom panel of Fig. 5). The increase in $\overline{m}$ occurs because, on average, low-mass stars acquire larger velocities during pericentre passages and are hence more likely to escape from the cluster. The value of r_h is seen to increase during the perigalactic passage but rapidly settles back to a value slightly below the circular-

orbit value. Thus while the tidal shocks experienced by the clusters on elliptical orbits do not affect the evolution of R_c, they are nonetheless strong enough to modify other important properties of the cluster. As Fig. 5 shows, the impact of the shocks on the cluster properties increases with time – this is due to the decreasing number of bound stars in the cluster.

3.3 Strength of tidal shocks

Before drawing our final conclusions based on these simulations, we now investigate whether the lack of impact on R_c is due to the weakness of the shocks we have simulated or whether the value of R_c is intrinsically robust to tidal shocking. The strength of a tidal shock is generally presented in terms of the dimensionless parameter β_{sh} given by (e.g. Spitzer 1987)

$$\beta_{sh} = \frac{t_{rh}}{t_{sh}}, \tag{5}$$

where t_{sh} is an estimate of the destruction time of the cluster owing to energy input from the gravitational shocks. The time scale t_{sh} is given by

$$t_{sh} = \frac{|E_h|}{dE_h/dt}, \tag{6}$$

where E_h is the energy of the cluster evaluated at the half-mass radius and dE_h/dt is the rate at which stars at the half-mass radius acquire energy due to the shock. In a simulation containing a finite number of stars, evaluation of this expression requires some care. Averaging the energy changes of stars near the half-mass radius does not produce robust results because individual stars may gain and lose energy during the perigalactic passage through other means than interaction with the external tidal field. Instead we calculate the total energy binding the cluster as a function of time and estimate the energy input to the cluster during perigalactic passages. Fig. 6 compares the time evolution of the binding energy E_b of a cluster on a circular orbit with that of a cluster on an elliptical orbit. For a cluster in an external potential E_b is defined as (e.g. Fukushige & Heggie 1995)

$$E_b = T + V + E_T \tag{7}$$

where T and V are the total kinetic and potential energy of the cluster, respectively, and E_T is the energy in the tidal field. The binding energy must be negative for the cluster to remain bound. The effects of the external field are visible as dramatic changes in E_b at about 180 and 520 Myr. Note that the sudden, temporary change in E_b for the circular run at about 700 Myr is due to a collision between two binaries that results in the the break-up of one of the binaries and the subsequent ejection of its components. The ratio of the energy produced by this event to the binding energy of the cluster emphasises the relatively fragile nature of the clusters we are simulating.

During perigalactic passages, some stars acquire velocities above the escape velocity of the cluster and this leads to an enhanced mass-loss rate (see Fig. 7). However, the finite time required for such stars to escape means that E_b can temporarily become positive because it is calculated by summation over all stars within twice the tidal radius of the clus-
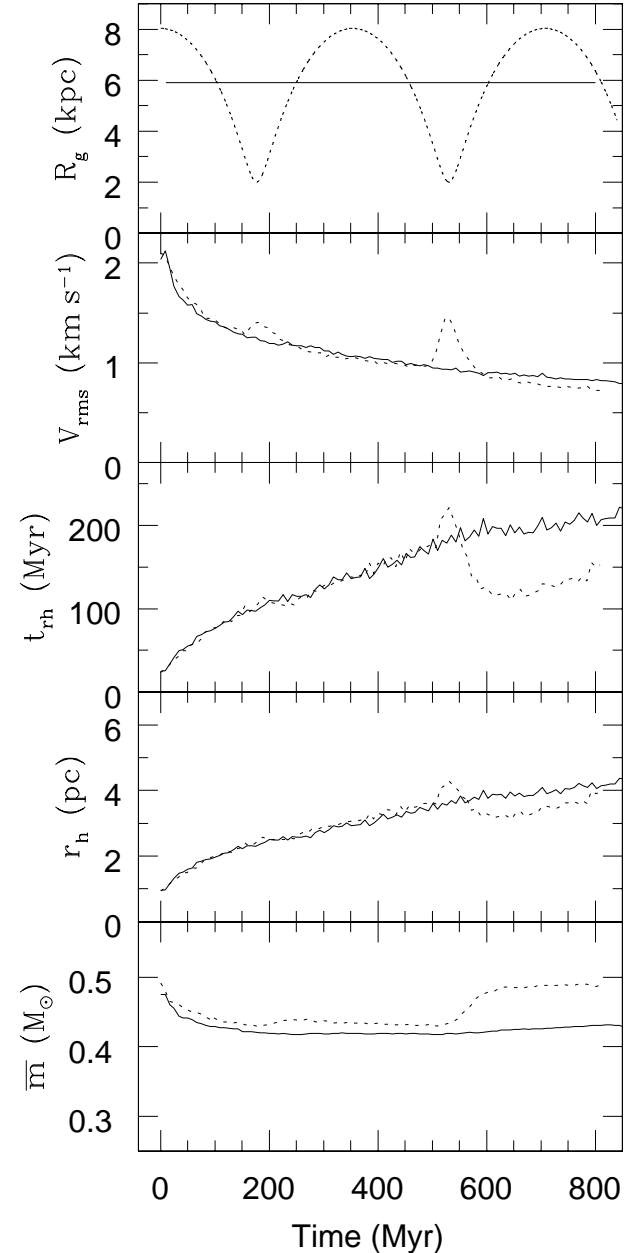

Figure 5. (Top panel) Variation of galactocentric radius R_g with time for a cluster on an elliptical orbit (broken curve). The solid line shows the position of the circular orbit of equal time-averaged radius. (Lower four panels) Evolution of rms velocity v_{rms}, half-mass relaxation time t_{rh}, half-mass radius r_h and mean stellar mass $\overline{m}$. Curves for two cases are shown: (1) a cluster on a circular orbit (solid curves) and (2) a cluster on an elliptical orbit (broken curves). Note that the half-mass radius is calculated using all stars within a radius of $2r_{t,a}$ of the cluster centre. In the simulations all such stars are classified as non-escapers, although at any given time a fraction of them are formally unbound.

ter. After the cluster has passed pericentre, stars continue to leave across the tidal boundary and E_b returns to a negative value indicating that the remaining cluster is still gravitationally bound. Following each shock, the cluster undergoes a revirialisation process during which the energy acquired from the tidal interaction is redistributed among the cluster
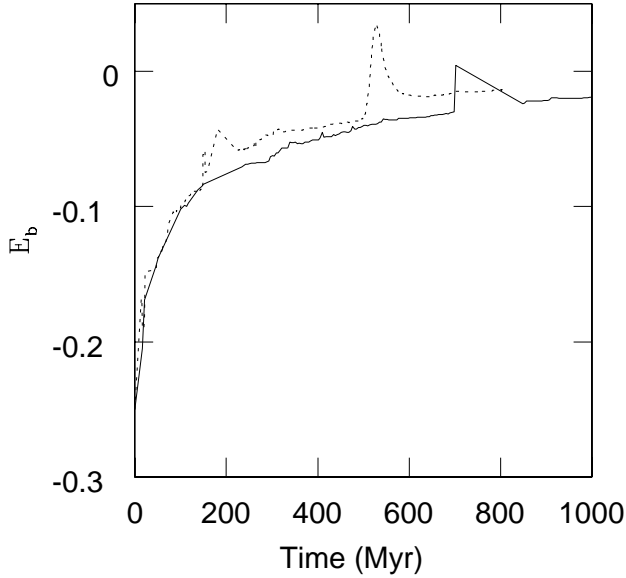
Figure 6. Evolution of the energy binding the cluster E_b. Curves for two cases are shown: (1) a cluster on a circular orbit (solid curve) and (2) a cluster on an elliptical orbit (broken curve). Energies are given in standard N-body units ($G = M_0 = 1, E_{b,0} = -1/4$).
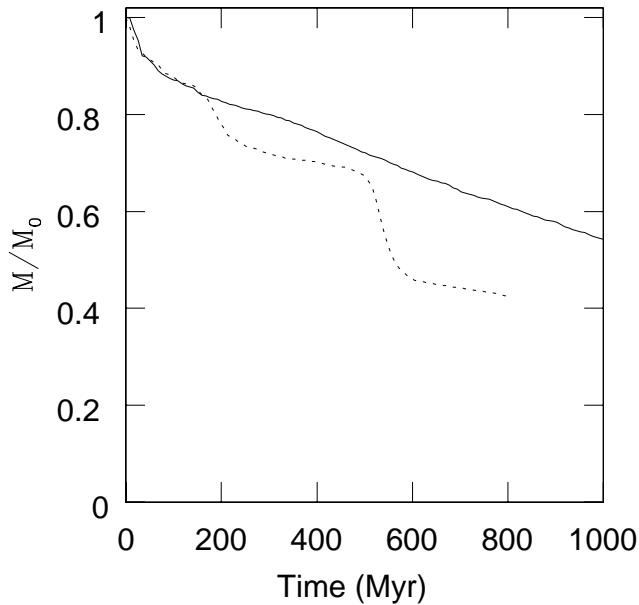

Figure 7. Evolution of total cluster mass M for clusters on circular (solid curve) and elliptical (broken curve) orbits in units of the initial mass M_0. Enhanced mass loss during the period of revirialisation which follows each perigalactic passage is seen in the elliptical orbit case.

stars. This process results in further loss of mass from the cluster because, on average, the revirialisation process gives velocity kicks to stars which are three times larger than those arising from the initial shock (see e.g. Gnedin & Ostriker 1999).
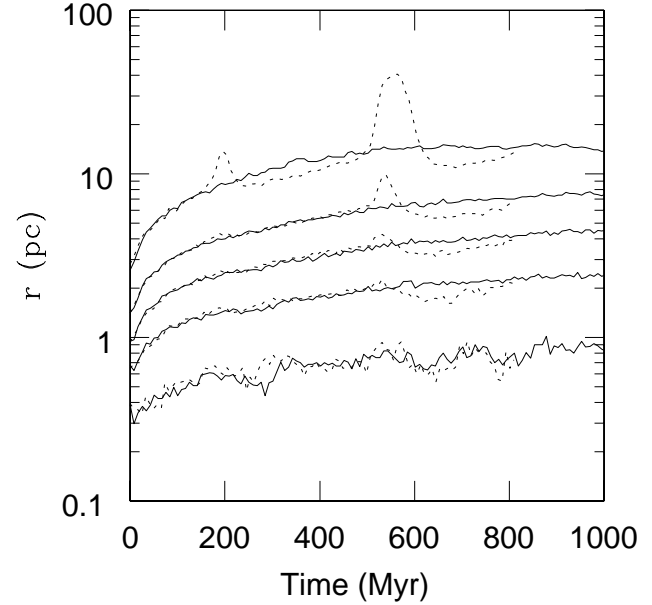

Figure 8. Evolution of the Lagrangian radii. Curves for two cases are shown (1) for a cluster on a circular orbit (solid curves) and (2) for a cluster on an elliptical orbit (broken curves). From bottom to top, the curves show the radii containing 10, 30, 50, 70 and 90 per cent of the cluster mass. The heating effect from the external tidal field is evident, even at the radius containing only 30 per cent of the cluster mass.

We take the energy input by the shock to be the difference between the energy of the cluster after this revirialisation process is complete and the energy of the cluster on the circular orbit at this time (about $T = 540$ Myr). The time between the shocks is 340 Myr, which leads to $t_{sh} \approx 6800$ Myr. At this time t_{rh} for the cluster is about 170 Myr, so the shock strength is about 0.02. Comparing this value with Fig. 13 of Gnedin et al. (1999) and noting that the initial concentrations $c = \log_{10}(r_t/r_d)$ of our clusters are about 1.1 (where we assume that r_t is the initial outer limit of the clusters), we find that our clusters lie approximately on the borderline of the region where shocks are important. We conclude that the shocks our clusters are experiencing would significantly affect their evolution on long time scales. Indeed, as Fig. 8 illustrates, even the 30 per cent Lagrangian radius of the cluster is affected by the tidal shocks, indicating energy input into the cluster over a wide range of radii. Nevertheless, on a timescale of up to 10^9 yrs, the effects of tidal heating are insufficient to modify the observed R_c of the clusters significantly.

3.4   Discussion

The top panel of Fig. 4 illustrates an important point which is worth emphasizing in the context of comparisons between simulated data and observations, namely that R_c and r_h are not, in general, related in a simple way. In particular circumstances, for example at the start of our simulations where the model clusters are in strict dynamical equilibrium, it is easy to show that, for a Plummer model composed of equal mass stars, the two quantities are related by $r_h = 2R_c$. However, Fig. 4 shows that this relation quickly breaks
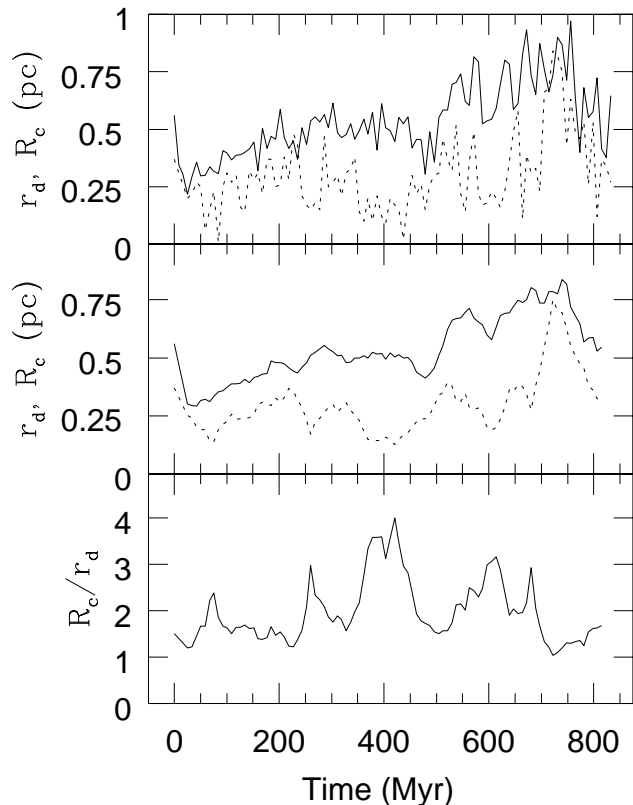
Figure 9. Comparison of the evolution of the density radius r_d (broken curve) with the observational core radius R_c (solid curve) for a single N-body cluster. Top: Un-smoothed results from the simulations. Middle: Curves smoothed by averaging over five time bins. Bottom: Ratio of R_c to r_d calculated using the smoothed curves from the middle panel. See text for discussion.

down as the cluster evolves away from its initial conditions. Thus, in the absence of further information, observational estimation of R_c must not be assumed to imply knowledge of the mass distribution in the cluster.

The same is true of the density radius r_d defined in Section 1. Fig. 9 shows the evolution of R_c (solid curve) and r_d (broken curve) for one of the clusters on an elliptical orbit. As the top panel of the figure shows, in a small-N simulation, both R_c and r_d are intrinsically noisy quantities: this is emphasised by the middle panel where we have smoothed the curves from the top panel using a window function of width five time bins. The bottom panel of Fig. 9, which shows the ratio of R_c to r_d for the smoothed data, demonstrates that the relation between the two quantities is not a simple proportionality and that the evolutionary trends in the two quantities can be quite different. The complicated relation between light and mass in star clusters is the result of a variety of processes such as stellar evolution and mass segregation which modify the mass and light distributions in different ways. Given the absence of simple relations between the different core radii, great care must be exercised when we interpret observational data through comparison with numerical simulations or theoretical models.

The simulations we have performed contain relatively low numbers of stars and are smaller and of lower total mass than the actual LMC clusters. However, the mean densities of our clusters are very similar to those of the LMC clusters and it is this which determines the extent to which an external tidal field can influence the internal dynamics of a cluster. On this basis, we can be confident that conclusions based on our simulations are relevant to the clusters in the LMC. Our simulations have shown that, on a timescale of 1 Gyr, which corresponds to several t_{rh} for our model clusters, tidal forces are not able to produce a spread in core radius similar to that observed among the LMC clusters.

There are two obvious avenues for building on the simulations we have performed. First, simulations of clusters containing a larger numbers of stars N could be performed. This would allow us to achieve cluster masses comparable to those of the real LMC clusters. However, increasing N in a cluster while holding the physical density of the cluster constant leads to an increase in t_{rh}. The expansion seen in R_c for our simulated clusters is driven primarily by two-body processes (which proceed on a time scale t_{rh}) rather than by tidal heating and it will therefore be slowed by increasing N. Further, the disruptive effect of pericentre passages depends on the ability of a cluster to re-fill the region outside its pericentric tidal radius $r_{t,p}$ during the time between close passages. As t_{rh} increases this re-filling is reduced. The cluster will therefore have fewer stars outside $r_{t,p}$ and hence will be less affected by shocks than small-N clusters (see Fig. 2 of Baumgardt & Makino (2003)). A cluster on an elliptical orbit and which, as in our simulations, initially filled its pericentric tidal radius would remain truncated at this radius throughout its evolution because there would not be sufficient time between perigalactic passages for the region outside $r_{t,p}$ to be re-filled (Oh & Lin 1992). Thus shocks should have less impact on the R_c of larger-N clusters and the observed expansions of clusters on both circular and elliptical orbits should remain similar.

The second possible improvement would be to use a more realistic model of the LMC potential, for example one based upon the recent mass models of van der Marel et al. (2002). However, the actual LMC mass distribution is more extended than the Keplerian potential we have been using in our simulations and therefore the gradients in its gravitational field are smaller. Consequently, the associated strength of its tidal effects on clusters moving on elliptical orbits is reduced.

Thus, we conclude that neither of the above modifications to our simulations would tend to increase the effect of the tidal field. The fact that the time-varying tidal field in our simulations did not result in changes in the evolution of R_c in the extreme case of a low-mass cluster in orbit about a point-mass galaxy leads us to conclude that tides have not yet had time to play a significant role in the internal evolution of the intermediate-age LMC clusters.

4 MODELS WITH PRIMORDIAL BINARIES

4.1 Steady tidal field case

In this section we present results for models moving in a steady tidal field but with different numbers of primordial binaries, in order to isolate the impact of large binary fractions on the evolution of the cluster properties. The clusters discussed here move on the same orbits as the circular orbit runs of Section 3.

Based on an analysis of the observed binary sequence in the young cluster NGC 1818, Elson et al. (1998) have shown that the binary fraction f_b in the centre of this cluster is about 0.35. Here $f_b = N_b/(N_s + N_b)$, where N_s and N_b are the numbers of single stars and binary systems, respectively. To date, the binary fractions of the older clusters in our sample have not been determined. Thus, at present the binary fractions of these clusters are essentially free parameters. Heggie's (1975) law implies that only hard binaries are dynamically important in the evolution of a star cluster. A binary is said to be hard when the magnitude of its binding energy $|E_{bin}|$ exceeds the kinetic energy of a typical cluster star (Heggie 1975). In the case of a binary with component masses m_1 and m_2 at a separation a moving in a cluster with mean mass $\overline{m}$ and velocity dispersion σ the hardness condition is

$$\frac{Gm_1m_2}{2a} > \frac{1}{2}\overline{m}\sigma^2. \tag{8}$$

(We note that the NBODY4 code uses a dispersion of $\sqrt{2}\sigma$ in this equation to determine the hardness limit for binaries, in order to take account of the larger velocity dispersion in the core of a centrally concentrated cluster.) In our simulations the boundary between hard and soft binaries occurs at a separation of about 120 AU for binaries containing stars of the mean stellar mass in the cluster. Hard binaries act as heat sources because they become more tightly bound as a result of interactions with single stars and thereby impart kinetic energy to the stars they encounter. Heggie & Aarseth (1992) found that the density radii of clusters containing primordial binaries experienced shallower contraction during core collapse and subsequently tended to be larger than those of clusters containing only single stars. This result, based on simulations of single-mass clusters with binary fractions of about 0.03, motivates our investigation of clusters containing large numbers of primordial binaries. Hereinafter, we will use f_b to refer to the fraction of *hard* binaries in the cluster.

As an extreme case, we consider first clusters with initial $f_b = 0.5$ and with the hard binaries randomly distributed throughout the cluster. In each binary the mass of the primary star is drawn from the IMF of Kroupa et al. (1993) and the mass of its companion is obtained by randomly choosing a mass ratio for the binary from a uniform distribution constrained by the single star mass limits (for a more detailed discussion, see Hurley et al. 2001). The binary orbital parameters are generated from the distribution of Eggleton et al. (1989). The clusters are otherwise generated exactly as in the single star runs of Section 3. We note that the inclusion of a large number of hard primordial binaries dramatically increases the computation time required for each simulation.

Fig. 10 compares the evolution of R_c for clusters containing $N = 5000$ single stars and no primordial binaries with that for clusters containing a significant initial binary population. An increased binary fraction produces a noticeable effect on the evolution of R_c. After 1 Gyr, the core radii of clusters containing 50 per cent primordial binaries are about a factor of two larger than those of clusters with no binaries.

The results presented in Fig. 11 give some insight into the mechanism by which a large binary fraction can drive an expansion of R_c. The top panel shows that the rate at
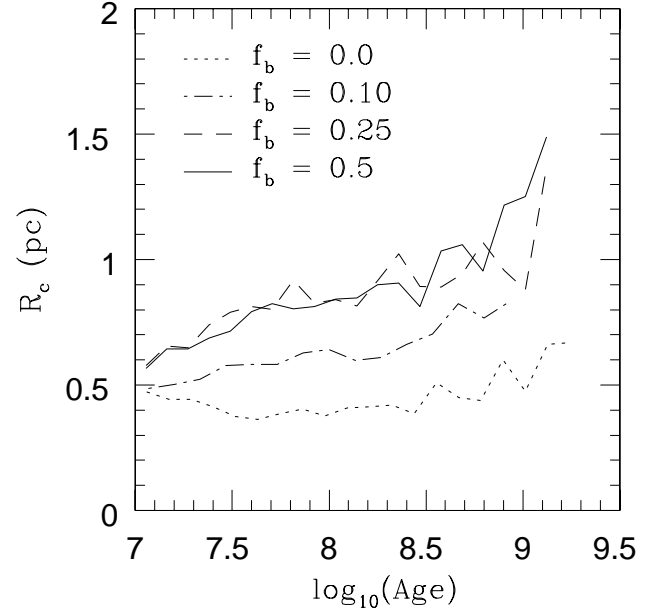

Figure 10. Core radius evolution for *N*-body clusters containing single stars only (short-dashed curve) and clusters containing 10 per cent, 25 per cent and 50 per cent hard primordial binaries (short-long dashed, long-dashed and solid curves, respectively). All clusters are on circular orbits about the LMC. See text for discussion.

which mass is lost from a cluster with initial $f_b = 0.5$ is significantly greater than in the case of a cluster with no initial binary population. After 1 Gyr this cluster has lost almost 25 per cent more mass than the cluster containing only single stars. The evolution of the energy binding the cluster E_b is shown in the second panel of Fig. 11. In a cluster with a large initial binary fraction, E_b rapidly attains a value significantly higher than that of a cluster of single stars. The enhanced mass-loss rate due to the presence of the binaries decreases the depth of the cluster's potential-well; the magnitude of the binding energy is further reduced by the heating of the remaining bound stars through weak encounters. As Fig. 12 shows, the energy input due to binary heating is distributed throughout the cluster. All the Lagrangian radii of the cluster rapidly attain larger values when the cluster contains primordial binaries. We note that, as was discussed in Section 3.2, the growth of the clusters containing only single stars is due to the fact that the clusters do not fill their tidal radii at the start of the simulations. We use identical initial conditions for the clusters containing binaries – the excess heating observed in those clusters is due to the presence of the hard binary population.

The third panel of Fig. 11 shows the internal binding energy of the primordial hard binaries E_{bin} as a function of time. In calculating E_{bin} we include the binding energy of those hard binaries which have escaped from the cluster because we are interested in the rate at which encounters lead to the hardening of binaries. This plot demonstrates that, as expected, the hard binaries become harder with time and so impart energy to the cluster. It is well known that energy generation by hard binaries halts core collapse (e.g. Heggie & Aarseth 1992). However, Fig. 11 demonstrates that even in the very early stages of a cluster's evolution, the
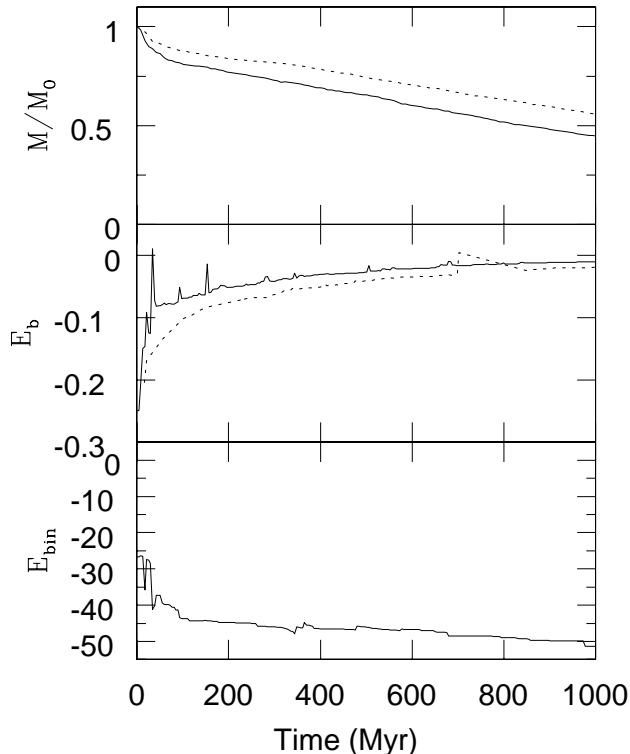
Figure 11. Comparison of the evolution of the total cluster mass M (top panel) and the energy binding the cluster E_b (middle panel). Two cases are shown (1) a cluster without primordial binaries (broken curves) and (2) a cluster containing 50 per cent primordial binaries (solid curves). The total mass is normalised by its initial value M_0 and E_b is given in standard N-body units. The bottom panel shows the evolution of the internal binding energy of the primordial binaries E_{bin} (in standard N-body units) in the run containing primordial binaries. The decrease in E_{bin} is the result of interaction-induced binary hardening. Note that E_{bin} includes the internal energy of escaped binaries. See text for discussion.
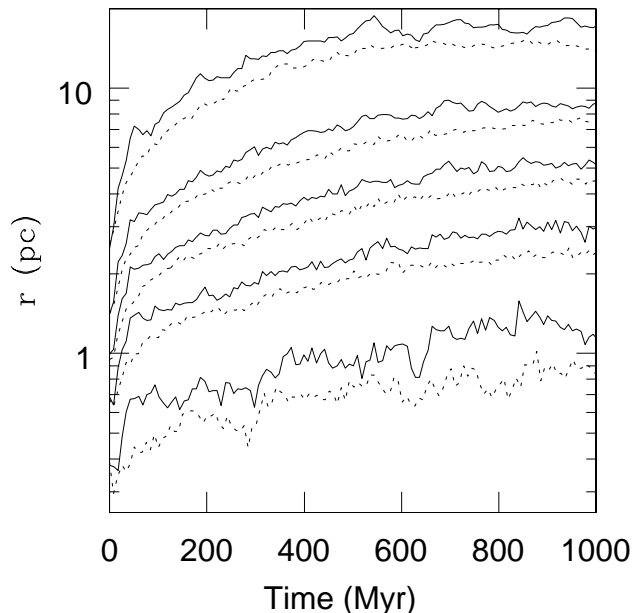

Figure 12. Evolution of the Lagrangian radii for clusters with 50 per cent primordial binaries (solid curves) and with single stars only (broken curves). From bottom to top, the curves show the radii containing 10, 30, 50, 70 and 90 per cent of the cluster mass. The heating effect of the primordial binaries is visible at all radii.

heating effect of a large primordial hard binary population can have a significant impact on the energy budget of the cluster.

We note that the occasional large changes in E_{bin} are the result of stellar evolutionary processes and therefore do not contribute to the direct heating of the cluster. For example, at $T = 34$ Myr the components of one binary system merge to form a single star: prior to the merger the binary is hardened by tidal interactions between its components. The massive star thus produced explodes as a supernova soon after and the velocity kick received by the remnant as a result of the explosion is reflected in the spike in E_b. The prominence of this event is due to the relatively small number of stars in the simulation.

Fig. 10 shows that the R_c evolution of clusters with $f_b = 0.25$ is very similar to that of clusters with $f_b = 0.5$ initially. This suggests that the heating effect of primordial binaries saturates above a certain value of the binary fraction $f_{b,crit}$. For larger values of f_b, the R_c evolution is unchanged, although the mass-loss rate is greater for increased f_b. From Fig. 10 we see that $f_{b,crit}$ for the clusters we have simulated appears to lie in the range $0.1 - 0.25$ because an

initial binary fraction of 10 per cent has a noticeably smaller impact on R_c than one of 25 per cent. We are currently investigating this effect in more detail, including its dependence on the number of stars in the simulation: the results will be presented elsewhere. Here we note only that the saturation may arise from the fact that at early times only a relatively small number of binaries take part in the heating process. In our simulations only about three per cent of the binaries are dynamically hardened during the first 100 Myr. We find that this fraction appears to be independent of the value of f_b. Whether a particular binary experiences an encounter which leads to hardening depends on the masses and separation of the components as well as the local stellar density in the neighbourhood of the binary. For a fixed binary mass, however, the hardest binaries have the smallest separations and hence are least likely to interact with other stars. This is reflected in our simulations: for a given binary mass, all the binaries which undergo early hardening are initially among the more weakly bound pairs.

4.2 Time-varying tidal field case

In our final set of simulations we examine clusters containing large numbers of primordial binaries and moving on non-circular orbits about the LMC. We have considered the extreme case of $f_b = 0.5$ but, as was shown in the previous section, these results also apply to somewhat smaller values of f_b. As Fig. 13 shows, the core radius of a cluster on an elliptical orbit and containing primordial binaries exhibits stronger growth than that of a cluster of single stars on a circular orbit: after about 600 Myr the core radius of the former cluster is almost a factor of two larger. The increase in core radius is solely due to the presence of binaries. As in
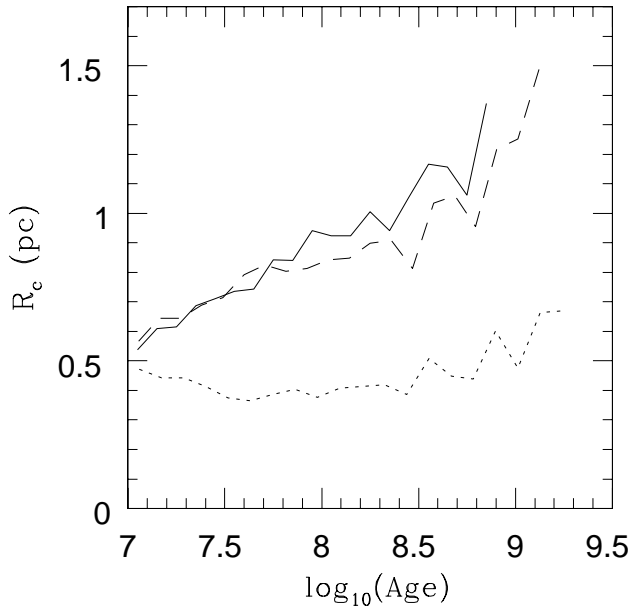
Figure 13. Core radius evolution for N-body simulations of clusters on different orbits about a point mass representing the LMC with (solid and long-dashed curves) and without (short-dashed curve) hard primordial binaries. The solid curve represents a cluster on an elliptical orbit, while both broken curves represent clusters on circular orbits. See text for discussion.

the case of clusters containing only single stars (Section 3), a cluster with the same primordial binary fraction but on a circular orbit exhibits almost identical core radius evolution. However, the increased mass-loss rate which results from binary heating leaves the cluster on the elliptical orbit more vulnerable to tidal disruption. After only 600 Myr, the cluster has lost almost 75 per cent of its mass and the core radius determination is consequently very uncertain. By 1 Gyr it is virtually disrupted and retains only about 10 per cent of its initial mass while the circular orbit cluster still contains about 45 per cent of its initial mass.

4.3   Discussion

Our simulations demonstrate that the presence of a large population of hard binaries can produce significant expansion of the core radius of a cluster. In agreement with many previous studies (e.g. Spitzer & Mathieu 1980; Heggie & Aarseth 1992; de La Fuente Marcos 1996) we have thus shown that binaries constitute a dynamically significant population in star clusters. In particular, we have found that primordial binaries can rapidly affect observable cluster properties such as R_c. In the context of the LMC clusters, however, it is clear that the presence of binaries alone cannot account for the the observed trends in R_c and in particular for the factor of three difference in core radius between NGC 1831 and NGC 1868. Even in the extreme case in which one cluster has no primordial binaries at all while the other cluster has a hard binary fraction of $25-50$ per cent, the difference in R_c over the lifetime of the intermediate-age clusters is at most a factor of two. The core radius of a cluster containing 10 per cent binaries expands by only a factor of 1.5 over the same time scale. Further, the similarity of the ob-

served present-day luminosity functions of the clusters in the GO7307 sample (de Grijs et al. 2002b) argues against large inter-cluster variations in the IMF and hence makes significant differences in binary fraction unlikely.

The initial radial distribution of hard binaries has an impact on their heating effect on the cluster stars (e.g. de La Fuente Marcos 1996) and may also have a bearing on the saturation of the heating effect which we observed in Section 4.1. A binary population which was more centrally concentrated than the single stars as a result of either primordial or dynamical mass segregation would be expected to produce more heating because of the increased interaction rates in the inner parts of the cluster. In our future simulations we will consider alternatives to the uniform distribution used in the present runs. However, based on our current simulations it is possible to estimate the significance of centrally concentrating the binary population. The clusters with 50 per cent binary fractions contain approximately the same number of binaries within R_c as a cluster with a 10 per cent overall binary fraction in which all the binaries are located within R_c. Given that none of our simulations exhibited R_c growth of a magnitude sufficient to match the observations, a core binary fraction in excess of 50 per cent would be required to produce greater R_c growth. The observed similarity of the degree of mass segregation in the intermediate-age clusters (de Grijs et al. 2002b) render it unlikely that the radial distribution of binaries could vary so greatly between clusters.

As in the case of the simulations in Section 3, it is natural to ask whether our conclusions are also valid for clusters containing larger numbers of stars than those in our current simulations. The simulation of large-N clusters containing significant numbers of primordial binaries has only recently become feasible and we are currently investigating the impact of binaries on the evolution of such clusters; the results of this study will be presented elsewhere. The present simulations show that the disruption time for a small-N cluster in a time-varying external tidal field is significantly reduced if it contains a large fraction of primordial binaries. It is not trivial to extrapolate these results to larger-N clusters. However, binary heating of the cluster is essentially a two-body process and therefore proceeds on the relaxation time scale $t_{\rm rh}$. Given that a larger-N cluster with the same mean physical density has a larger $t_{\rm rh}$, the physical rate at which the cluster is heated by its binary population will be reduced. Thus, while larger-N clusters would obviously survive for longer than those in our present simulations, their physical rate of R_c expansion would be reduced. Large variations in primordial binary fraction are therefore unlikely to be the explanation of the LMC observations.

5   CONCLUSIONS

The core radii of star clusters in the LMC display a strong trend with age, namely that the older clusters exhibit a much greater spread in core radius than their younger counterparts. In particular, the R_c of the intermediate-age clusters NGC 1868 and NGC 1831 differ by about a factor of three. It has been suggested (Elson et al. 1989; Mackey & Gilmore 2003) that the trend represents a physical evolution of the clusters and that the clusters all formed with similar, small
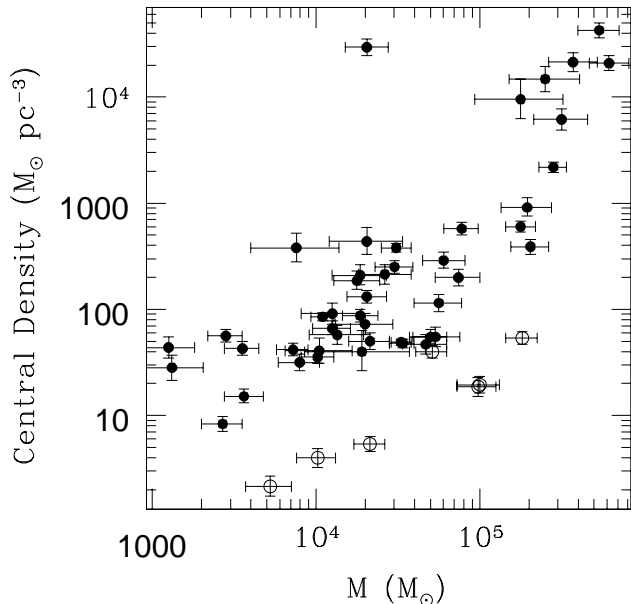
Figure 14. Plot of central mass density versus estimated mass M for the LMC cluster sample. Clusters with R_c larger (smaller) than 4 pc are shown as open (filled) circles. Data are taken from Mackey & Gilmore (2003).

core radii which were modified by subsequent dynamical evolution. The possibility that this might be caused by variations in the cluster IMF has been ruled out based on HST photometry of a sample of eight clusters (de Grijs et al. 2002b). In this paper we have used N-body simulations of star clusters initially containing up to $N = 5000$ stars to investigate some possible alternative explanations. We have considered two possible dynamical effects which could produce significant R_c evolution: time-varying external tidal fields and a varying population of primordial binaries.

Throughout this paper we have analysed our simulations using the same procedures as were applied by Mackey & Gilmore (2003) to the observed data. We emphasised the importance of such an approach by comparing the evolution of the observational core radius to that of the half-mass radius and the density radius. As has been pointed out by a number of authors (e.g. Portegies Zwart et al. 2001), in general there are no simple relations between these quantities. Thus observations of simulated data sets are essential to ensure that comparisons between observed and simulated data are made in a consistent manner.

We considered clusters on circular and elliptical orbits of equal time-averaged radius about a point mass representing the LMC. The clusters are scaled so that their limiting radii correspond to the pericentric tidal radius of the clusters on elliptical orbits. However, at the start of each simulation the clusters lie well within the tidal radius which corresponds to their initial galactocentric position (apocentre for the clusters on elliptical orbits and the circular radius for the clusters on circular orbits). Initially, the clusters expand due to stellar mass loss but the competing effect of mass segregation means that R_c decreases slightly. At later times, two-body relaxation processes drive a further expansion of the clusters because the clusters are not tidally limited. This

expansion is mirrored by a growth in R_c. However, the rate of R_c expansion is found to be identical irrespective of the orbit on which the cluster is moving. We conclude that differences in the cluster orbits cannot be responsible for the observed differences in R_c among the LMC clusters.

Given that the binary fractions of all but the youngest clusters are currently unconstrained by observations, we compared the evolution of the R_c of a cluster containing no primordial binaries with that of a cluster with a large initial hard binary fraction. The presence of significant numbers of binaries leads to increased growth of R_c compared with the evolution of clusters containing only single stars. Binary fractions of 50 per cent and 25 per cent produce similar degrees of R_c expansion, while a 10 per cent binary fraction results in noticeably less growth. Even in the most extreme case of a cluster with a binary fraction of 50 per cent on an elliptical orbit, however, R_c increases by at most a factor of two. Not only is this smaller than the increase required to explain the LMC observations but the required spread in primordial binary fraction is already difficult to reconcile with the observed similarity of the cluster stellar luminosity functions (de Grijs et al. 2002b).

Our simulations have demonstrated that neither large variations in primordial binary fraction nor differences in cluster orbits about the LMC can account for the R_c–age relation seen in the LMC clusters. The origin of the spread in R_c among the intermediate-age clusters therefore remains an open issue. We now return briefly to the observed data on the LMC cluster system as a whole to see whether there are any further clues to the origin of the trend.

Fig. 14 presents evidence for a systematic difference in the central density of the large-R_c clusters relative to the rest of the cluster population: these clusters have systematically lower central densities for a given cluster mass. This could be indicative of variations in star formation efficiency (SFE) between the clusters: low SFE leads to rapid cluster expansion and consequently a drop in the central density (e.g. Goodwin 1997). Simulations of cluster expansion due to residual gas expulsion from clusters with low SFE (Goodwin 1997) do not appear to show sustained core expansion of the magnitude seen in the intermediate-age LMC clusters. However, the core radii quoted in Goodwin (1997) are those of the mass distribution in the simulated clusters which, as was discussed in Section 3, may not accurately reflect the changes in the light distribution. We are currently investigating the long-term evolution of clusters which experience different degrees of primordial gas loss owing to SFEs in the range $0.25 - 0.60$, required to explain the range of core radii seen in the youngest LMC clusters (Goodwin 1997). We are also simulating the effects of primordial binaries on larger-N clusters. Of particular interest is the possibility that the heating effects of a large binary population could enable a cluster to retain a large initial R_c produced by gas expulsion.

REFERENCES

Aarseth S.J., 1999, Celestial Mechanics and Dynamical Astronomy, 73, 127

Aarseth S.J., 2001, New Astronomy, 6, 277

Aarseth S.J., Heggie D.C., 1998, MNRAS, 297, 794

Aarseth S.J., Hénon M., Wielen R., 1974, A&A, 37, 183

Baumgardt H., 1998, A&A, 330, 480

Baumgardt H., 2001, MNRAS, 325, 1323

Baumgardt H., Hut P., Heggie D.C., 2002, MNRAS, 336, 1069

Baumgardt H., Makino J., 2003, MNRAS, 340, 227

Beaulieu S.F., Elson R., Gilmore G., Johnson R.A., Tanvir N., Santiago B., 1999, in IAU Symp. 190: New Views of the Magellanic Clouds, vol. 190, 460

Binney J., Tremaine S., 1987, Galactic dynamics, Princeton University Press, Princeton, NJ

Bonnell I.A., Bate M.R., Clarke C.J., Pringle J.E., 2001, MNRAS, 323, 785

Casertano S., Hut P., 1985, ApJ, 298, 80

de Grijs R., Gilmore G.F., Johnson R.A., Mackey A.D., 2002a, MNRAS, 331, 245

de Grijs R., Gilmore G.F., Mackey A.D., Wilkinson M.I., Beaulieu S.F., Johnson R.A., Santiago B.X., 2002b, MNRAS, 337, 597

de La Fuente Marcos R., 1996, A&A, 314, 453

Eggleton P.P., Fitchett M.J., Tout C.A., 1989, ApJ, 347, 998

Elson R.A.W., 1991, ApJS, 76, 185

Elson R.A.W., 2000, in Martinez Roger C., Sanchez F., Perez Fournon I., eds., Globular Clusters, Cambridge University Press, Proceedings of the Xth Canary Islands Winter School, 209

Elson R.A.W., Fall S.M., Freeman K.C., 1987, ApJ, 323, 54

Elson R.A.W., Freeman K.C., Lauer T.R., 1989, ApJ, 347, L69

Elson R.A.W., Sigurdsson S., Davies M., Hurley J., Gilmore G., 1998, MNRAS, 300, 857

Fall S.M., Zhang Q., 2001, ApJ, 561, 751

Fukushige T., Heggie D.C., 1995, MNRAS, 276, 206

Giersz M., Heggie D.C., 1997, MNRAS, 286, 709

Gnedin O.Y., Lee H.M., Ostriker J.P., 1999, ApJ, 522, 935

Gnedin O.Y., Ostriker J.P., 1997, ApJ, 474, 223

Gnedin O.Y., Ostriker J.P., 1999, ApJ, 513, 626

Goodwin S.P., 1997, MNRAS, 286, 669

Heggie D.C., 1975, MNRAS, 173, 729

Heggie D.C., 2001, in The Restless Universe: Applications of Gravitational N-Body Dynamics to Planetary, Stellar and Galactic Systems, Institute of Physics Publishing, Bristol, 109

Heggie D.C., Aarseth S.J., 1992, MNRAS, 257, 513

Heggie D.C., Mathieu R.D., 1986, Lecture Notes in Physics Vol. 267: The Use of Supercomputers in Stellar Dynamics, 233

Hillenbrand L.A., 1997, AJ, 113, 1733

Hills J.G., 1980, ApJ, 235, 986

Hurley J.R., Pols O.R., Tout C.A., 2000, MNRAS, 315, 543

Hurley J.R., Tout C.A., Aarseth S.J., Pols O.R., 2001, MNRAS, 323, 630

Hurley J.R., Tout C.A., Pols O.R., 2002, MNRAS, 329, 897

Johnson R.A., Beaulieu S.F., Gilmore G.F., Hurley J., Santiago B.X., Tanvir N.R., Elson R.A.W., 2001, MNRAS, 324, 367

King I., 1962, AJ, 67, 471

King I.R., 1966, AJ, 71, 64

Kroupa P., Tout C.A., Gilmore G., 1993, MNRAS, 262, 545

Leon S., Meylan G., Combes F., 2000, A&A, 359, 907

Mackey A.D., Gilmore G., 2003, MNRAS, 338, 85

Makino J., Taiji M., Ebisuzaki T., Sugimoto D., 1997, ApJ, 480, 432

Meylan G., Heggie D.C., 1997, A&AR, 8, 1

Mikkola S., Aarseth S.J., 1993, Celestial Mechanics and Dynamical Astronomy, 57, 439

Mikkola S., Aarseth S.J., 1998, New Astronomy, 3, 309

Odenkirchen M., et al., 2001, ApJ, 548, L165

Oh K.S., Lin D.N.C., 1992, ApJ, 386, 519

Plummer H.C., 1911, MNRAS, 71, 460

Portegies Zwart S.F., Makino J., McMillan S.L.W., Hut P., 2002, ApJ, 565, 265

Portegies Zwart S.F., McMillan S.L.W., Hut P., Makino J., 2001, MNRAS, 321, 199

Spitzer L., 1987, Dynamical evolution of globular clusters, Princeton, NJ, Princeton University Press, 1987

Spitzer L., Mathieu R.D., 1980, ApJ, 241, 618

van der Marel R.P., Alves D.R., Hardy E., Suntzeff N.B., 2002, AJ, 124, 2639

Vesperini E., 1998, MNRAS, 299, 1019

Vesperini E., Heggie D.C., 1997, MNRAS, 289, 898

Zhao H., Evans N.W., 2000, ApJ, 545, L35